PNAS
www.pnas.org

Supplementary Information for

Modulation of the Hippo pathway and organ growth by RNA processing proteins

Jana Mach, Mardelle Atkins, Kathleen M. Gajewski, Violaine Mottier-Pavie, Leticia Sansores-Garcia, Jun Xie, Robert Andrew Mills, Weronika Kowalczyk, Leen Van Huffel, Gordon B. Mills, and Georg Halder

Georg Halder
Email: georg.halder@vib.be

This PDF file includes:

www.pnas.org/cgi/doi/10.1073/pnas.1807325115

SI Materials and Methods

Fly Stocks and Husbandry. The UAS-rPKCζ* fly line was described previously (1). The *GMR-GAL4, UAS-rPKCζ*/ CyO-GFP* tester stock was made via standard recombination techniques. Fly stocks were obtained from the Vienna Drosophila Resource Center: *UAS-Hrb27C*^{RNAi} (v16040 and v16041, v101555), *UAS-hpo*^{RNAi} (v104169), *UAS-wts*^{RNAi} (v106174), *UAS-sqd*^{RNAi} (v32395); or from Bloomington Stock Center: *diap1-lacZ* (12093), *myc-lacZ* (11981), *Dll-lacZ* (10981); *UAS-yki*^{V5} (28819), *UAS-yki*$^{S168A-V5}$ (28818), *UAS-sd*^{RNAi} (29352); *UAS-glo*^{RNAi} (36066), *UAS-hfp*^{RNAi} (34785), and *UAS-white*^{RNAi} (25787) which was used as a control RNAi; *UAS-Hrb27C*^{FLAG} was a gift from T. Yano, *UAS-sd*^{GA} was a gift from J. Jiang. The *DE-Gal4* line has been described previously (2). The driver lines *GMR-Gal4*, *dpp-Gal4*, *ptc-Gal4* and *hh-Gal4* were obtained from Bloomington Drosophila Stock Center. Mutant clones were induced using the FLP-FRT system and *ubi-GFP* marked chromosomes as described previously (3). The mutant alleles *Hrb27*^{J6} and *Hrb27C*$^{F2-1}$ were obtained by EMS mutagenesis. All fly crosses were reared using standard techniques at 25°C, unless specified otherwise. Heat-shocks were performed for 30 minutes at 37°C, 48 hours after egg deposition.

EMS mutagenesis and establishment of mutant stocks. In order to generate fly lines harboring random point mutations, we mutagenized the sperm of isogenized wild type males by feeding the chemical mutagen EMS and crossed them in bulk to *GMR-Gal4, UAS-rPKCζ** females. We screened roughly 100,000 F1 animals for suppression of the *rPKCζ** induced eye phenotype (for scheme of crosses, see Fig. S1A) and isolated 49 lethal suppressor mutations, which fell into 28 complementation groups. F1 progeny with suppressor phenotypes were individually backcrossed to the tester stock, and the F2 progeny scored again for a suppressor phenotype. Linkage determination of suppressor mutations was determined by standard genetic methods via further backcrosses of F2 males to the tester stock, and then balanced. To eliminate mutations that affect the activity of the *GMR* promoter or that generally rescue apoptosis, we tested whether suppressors also affected the phenotype caused by *GMR-Gal4* driven expression of the pro-apoptotic gene *hid*, which also causes a small eye phenotype (Fig.S1D). In this secondary screen, balanced mutant males were crossed to *GMR-Gal4, UAS-hid* females. Mutants that did not suppress the *GMR-Gal4, UAS-hid* small eye phenotype were scored as aPKC-specific suppressors. New mutations in *Hrb27C* were identified by complementation mapping to a second chromosome deficiency group (overlapping at 27C4 to 27C6) that suppressed the *GMR-Gal4, UAS-rPKCζ**, but did not modify *GMR-Gal4, UAS-hid* (Fig.1E-F, and Fig.S1D-G). Complementation tests with mutations in genes located in the overlap of the deficiencies and subsequent sequencing revealed that the suppressor mutants are new alleles of *Hrb27C*. Adults from the isogenized stock and larvae hemizygous for each new *Hrb27C* mutation were processed to make a crude genomic DNA template, and regions of the *Hrb27C* gene amplified via PCR. Sequencing of the PCR reactions uncovered a nonsense mutation at Gln247 for *Hrb27C*^{J6} and Trp239 for *Hrb27C*$^{F2-1}$.

Immunostaining of imaginal discs. Antibody stainings of imaginal discs were performed as described previously (4). Antibodies used: rabbit anti-Hrb27C (gift from D. Rio, 1:1000); mouse anti-βgalactosidase (Promega, 1:1000); mouse anti-CycE [Developmental Studies Hybridoma Bank at University of Iowa (DSHB), 1:40]; rat anti-ELAV (DSHB, 1:600); rabbit anti-Cleaved Caspase 3 (Cell Signaling, 9661S, 1:150), rat anti-Ci (DSHB, 1:150), mouse anti-Cut (DSHB, 1:100); rabbit anti-Yki (gift from K. Irvine, 1:10), guinea pig anti-Sens (gift from H. Bellen, 1:2000), mouse anti-Wg (DSHB, 1:100), mouse anti-24B10 (DSHB, 1:50). Secondary antibodies used: donkey anti-mouse Cy3 (Jackson ImmunoResearch, 1:500), donkey anti-rabbit Cy3 (Jackson ImmunoResearch, 1:500), donkey anti-rat Cy3 (Jackson ImmunoResearch, 1:500), donkey anti-guinea pig Cy3 (Jackson ImmunoResearch, 1:500), goat anti-mouse Cy5 (Jackson ImmunoResearch, 1:500), donkey anti-rabbit Cy5 (Jackson ImmunoResearch, 1:500). All samples

were stained with DAPI (1:2000). Imaginal discs were mounted in Vectashield (Vector Labs) and imaged on an Olympus FV1200 confocal microscope. Images were processed in ImageJ and Adobe software. Measurements for quantification were made in ImageJ using the Measure function and graphed with GraphPad Prism Software. One way ANOVA with a multiple comparisons analysis was performed with GraphPad Prism Software.

Cell culture. For luciferase assays we used the *Drosophila* cell line KC167 cultured in Schneider's medium containing 10% fetal bovine serum. 20,000 cells were seeded in a 48-well plate in presence of 2.5µg of the corresponding dsRNA. After 24hrs, cells were transiently transfected using Cellfectin II (Invitrogen) with the fusion construct *pRAc-Yki-GDBD* or *pRAc-Sc-GDBD*, and *pAc5.1-UAS-luc* (K. Basler) and *pRL-tub-Renilla* (K. Irvine) constructs. Luciferase assay was performed after 48hrs of DNA transfection using the Promega Dual-Glo kit. To produce dsRNA, we used specificity-tested primers from FlyBase Genome RNAi data base and fly gDNA as template for PCR and the Promega MEGAscript T7 kit.

Western Blot. Third instar larvae were dissected in cold PBS and eye imaginal discs were solubilized by boiling in 2x SDS sample buffer (125mM Tris-HCl pH6.8, 6% SDS, 20% glycerol, 0.025% bromophenol blue, and 10% β-Mercaptoethanol). Western blots were performed according to standard protocols. Antibodies used: anti-phospho-Yki and anti-Yki (generous gifts from Nic Tapon), anti-αTubulin (DSHB, Iowa).

Genotypes of animals shown in figures

Fig. 1.

A. *ex-lacZ / + ; dpp-Gal4 UAS-GFP / UAS-w^{RNAi}*
B. *ex-lacZ / UAS-aPKCζ* ; dpp-Gal4 UAS-GFP / UAS-w^{RNAi}*
C. *GMR-Gal4*
D. *GMR-Gal4 UAS-aPKCζ* / CyO-GFP*
E. *GMR-Gal4 UAS-aPKCζ* / Hrb27C^{J6}*
F. *GMR-Gal4 UAS-aPKCζ* / Hrb27C^{F2-1}*
G. *GMR-Gal4 UAS-aPKCζ* / Df(2L)BSC108*
H. *GMR-Gal4 UAS-aPKCζ* / UAS-Hrb27C^{RNAi}*

Fig. 2.

A. *ex-lacZ / + ; dpp-Gal4 UAS-GFP / UAS-Hrb27C^{RNAi}*
B. *ex-lacZ / UAS-aPKCζ*; dpp-Gal4 UAS-GFP / UAS-Hrb27C^{RNAi}*
C. *ex-lacZ / + ; hh-Gal4 UAS-GFP / UAS-w^{RNAi}*
D. *ex-lacZ / + ; hh-Gal4 UAS-GFP / UAS-Hrb27C^{RNAi}*
E. *ex-lacZ / + ; hh-Gal4 UAS-GFP / UAS-Hrb27C^{FLAG}*
F. *+ / + ; hh-Gal4 UAS-GFP / diap1-lacZ*
G. *UAS-Hrb27C^{RNAi} / + ; hh-Gal4 UAS-GFP / diap1-lacZ*
H. *Myc-lacZ / FM7c; + / + ; hh-Gal4 UAS-GFP / +*
I. *Myc-lacZ / + ; UAS-Hrb27C^{RNAi} / + ; hh-Gal4 UAS-GFP / +*
J. *ptc-Gal4 UAS-GFP / +*
K. *ptc-Gal4 UAS-GFP / UAS-Hrb27C^{RNAi}*
L. *ptc-Gal4 UAS-GFP / +*
M. *ptc-Gal4 UAS-GFP / UAS-Hrb27C^{RNAi}*
N. *ptc-Gal4 UAS-GFP / +*
O. *ptc-Gal4 UAS-GFP / UAS-Hrb27C^{RNAi}*

P. *Dll-lacZ / + ; hh-Gal4 UAS-GFP / +*
Q. *UAS-Hrb27C^{RNAi} / Dll-lacZ ; hh-Gal4 UAS-GFP / +*

Fig. 3.
A. *Hrb27C$^{F2\text{-}1}$ / CyO-RFP* and *Hrb27C$^{F2\text{-}1}$/ Df(2L)BSC108*
B. *y w ey-FLP; FRT40A ubi-GFP / FRT40A*
C. *y w ey-FLP; FRT40A ubi-GFP / Hrb27C^{J6} FRT40A*
D. *y w ey-FLP; FRT40A ubi-GFP / FRT40A*
E. *y w ey-FLP; FRT40A ubi-GFP / Hrb27C^{J6} FRT40A*
F. *ey-Gal4*
G. *ey-Gal4 / UAS-Hrb27C^{RNAi}*
H. *y w hs-FLP tub-Gal4 UAS-GFP; FRT40A Gal80 / Hrb27C^{J6} FRT40A*
I. *y w hs-FLP tub-Gal4 UAS-GFP; FRT40A Gal80 / FRT40A; Hrb27C^{RNAi} / +*
J. *y w hs-FLP tub-Gal4 UAS-GFP; FRT40A Gal80 / Hrb27C^{J6} FRT40A*

Fig. 4.
A. *ptc-Gal4 UAS-GFP ex-lacZ / + ; UAS-w^{RNAi} / +*
B. *ptc-Gal4 UAS-GFP ex-lacZ / + ; UAS-Hrb27C^{RNAi} / +*
C. *ptc-Gal4 UAS-GFP ex-lacZ / UAS-hpo^{RNAi} ; UAS-w^{RNAi} / +*
D. *ptc-Gal4 UAS-GFP ex-lacZ / UAS-hpo^{RNAi} ; UAS-Hrb27C^{RNAi} / +*
E. *ptc-Gal4 UAS-GFP ex-lacZ / UAS-wts^{RNAi} ; UAS-w^{RNAi} / +*
F. *ptc-Gal4 UAS-GFP ex-lacZ / UAS-wts^{RNAi} ; UAS-Hrb27C^{RNAi} / +*
G. *ptc-Gal4 UAS-GFP ex-lacZ / UAS-sd^{GA}; UAS-w^{RNAi} / +*
H. *ptc-Gal4 UAS-GFP ex-lacZ / UAS-sd^{GA}; UAS-Hrb27C^{RNAi} / +*
I. *ptc-Gal4 UAS-GFP ex-lacZ / + ; UAS-w^{RNAi} / UAS-yki$^{S168A\text{-}V5}$*
J. *ptc-Gal4 UAS-GFP ex-lacZ / + ; UAS-Hrb27C^{RNAi} / UAS-yki$^{S168A\text{-}V5}$*
K. *ptc-Gal4 UAS-GFP ex-lacZ / + ; UAS-w^{RNAi} / UAS-yki^{V5}*
L. *ptc-Gal4 UAS-GFP ex-lacZ / + ; UAS-Hrb27C^{RNAi} / UAS-yki^{V5}*
M. *ptc-Gal4 UAS-GFP ex-lacZ / UAS-wts^{RNAi}; UAS-w^{RNAi} / UAS-yki^{V5}*
N. *ptc-Gal4 UAS-GFP ex-lacZ / UAS-wts^{RNAi}; UAS-Hrb27C^{RNAi} / UAS-yki^{V5}*
O. *ptc-Gal4 UAS-GFP ex-lacZ / + ; UAS-Hrb27C^{RNAi} / +*

Fig. 5.
A. *ex-lacZ / UAS-sqd^{RNAi}; hh-Gal4 UAS-GFP / +*
B. *ex-lacZ / UAS-sqd^{RNAi}; hh-Gal4 UAS-GFP / UAS-Hrb27C^{RNAi}*
C. *ex-lacZ / UAS-glo^{RNAi}; hh-Gal4 UAS-GFP / +*
D. *ex-lacZ / UAS-glo^{RNAi}; hh-Gal4 UAS-GFP / UAS-Hrb27C^{RNAi}*
E. *ex-lacZ / UAS-Pabp2^{RNAi}; hh-Gal4 UAS-GFP / +*
F. *ex-lacZ / UAS-Pabp2^{RNAi}; hh-Gal4 UAS-GFP / UAS-Hrb27C^{RNAi}*
G. *ex-lacZ / + ; hh-Gal4 UAS-GFP / UAS-hfp^{RNAi}*
H. *ex-lacZ / + ; hh-Gal4 UAS-GFP UAS-hfp^{RNAi} / UAS-Hrb27C^{RNAi}*

Fig. S1.
A. *GMR-Gal4 UAS-aPKCζ* / CyO-GFP*
B. *GMR-Gal4 UAS-aPKCζ* / + ; UAS-sd^{RNAi} / +*
D. *GMR-Gal4 UAS-hid / +*
E. *GMR-Gal4 UAS-hid / Hrb27C^{J6}*
F. *GMR-Gal4 UAS-hid / Hrb27C$^{F1\text{-}2}$*
G. *GMR-Gal4 UAS-hid / K3-1*

Fig. S2.

A. *y w ey-FLP; FRT40A ubi-GFP / Hrb27C$^{F2\text{-}1}$ FRT40A*
B. *UAS-Hrb27C^{RNAi} / + ; DE-Gal4 / +*
C. *UAS-Hrb27C^{RNAi} / + ; DE-Gal4 / +*
D. *DE-Gal4 / +*
E. *UAS-Hrb27C^{RNAi} / + ; DE-Gal4 / +*
F. *+ / + ; hh-Gal4 UAS-GFP / UAS-Hrb27C^{RNAi}*
G. *ptc-Gal4 UAS-GFP / + ; UAS-Hrb27C^{RNAi} / +*
H. *ptc-Gal4 UAS-GFP ex-lacZ / UAS-lacZ; UAS-w^{RNAi} / +*
I. *ptc-Gal4 UAS-GFP ex-lacZ / UAS-lacZ; UAS-Hrb27C^{RNAi} / +*

Fig. S3.

A. *ex-lacZ / + ; hh-Gal4 UAS-GFP / UAS-w^{RNAi}*
B. *ex-lacZ / + ; hh-Gal4 UAS-GFP / UAS-Hrb27C^{RNAi}*
C. *ptc-Gal4 UAS-GFP / + ; UAS-w^{RNAi} / +*
D. *ptc-Gal4 UAS-GFP / + ; UAS-Hrb27C^{RNAi} / +*
E. *y w ey-FLP; FRT40A ubi-GFP / Hrb27C^{J6} FRT40A*
F. *y w ey-FLP; FRT40A ubi-GFP / Hrb27C^{J6} FRT40A*

Fig. S4.

A. *y w hs-FLP tub-Gal4 UAS-GFP; FRT40A Gal80 / Hrb27C^{J6} FRT40A*
B. *+ / + ; hh-Gal4 UAS-GFP / UAS-Hrb27C^{RNAi}*

Fig. S6.

ex-lacZ / ex-lacZ; hh-Gal4 UAS-GFP / TM6B or *ex-lacZ ptc-Gal4 UAS-GFP / CyO* crossed to various RNAi lines as indicated on the figure and the figure legend.

Fig. S7.

A. *ex-lacZ / UAS-sqd^{RNAi}; hh-Gal4 UAS-GFP / +*
B. *ex-lacZ / UAS-glo^{RNAi}; hh-Gal4 UAS-GFP / +*
C. *ex-lacZ / + ; hh-Gal4 UAS-GFP / UAS-hfp^{RNAi}*
D. *ex-lacZ / UAS-Pabp2^{RNAi}; hh-Gal4 UAS-GFP / +*

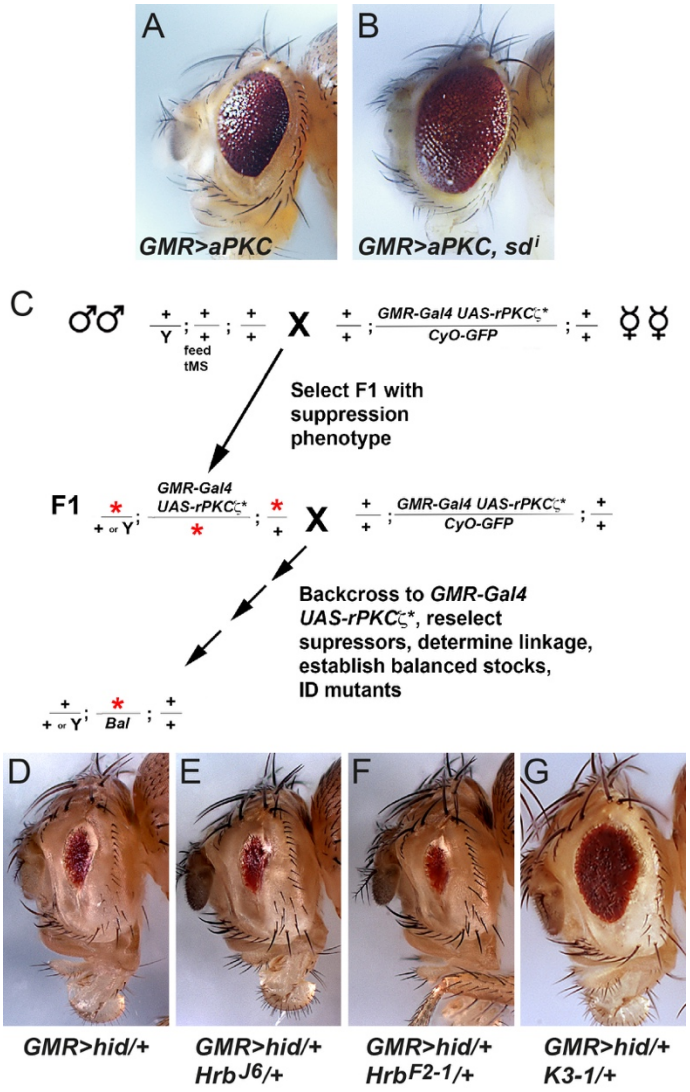

Figure S1. Crossing scheme of the aPKC suppressor screen and secondary screen for suppressors of apoptosis.
(A) Head of a fly with one copy of *GMR>aPKC.* (B) Head of a fly with one copy of *GMR>aPKC* and *UAS-sd*^{RNAi}. Note that these flies have a weaker *GMR>aPKC* induced eye phenotype than the screening stock presented in Figure 1 because this stock had already accumulated second site suppressors by the time this experiment was done. (C) Crossing scheme used to generate, screen, and isolate EMS induced mutations that suppress the aPKC overexpression eye phenotype. (D) Eye of a control fly with one copy of *GMR>hid.* (E-G) Eyes of flies with one copy of *GMR>hid* and one copy of *Hrb27C*^{J6}, *Hrb27C*$^{F2-1}$, or the unassociated *K3-1* suppressor mutation, which suppresses the cell death dependent small eye phenotype induced by *GMR>hid*, as an example of a non-specific aPKC suppressor.

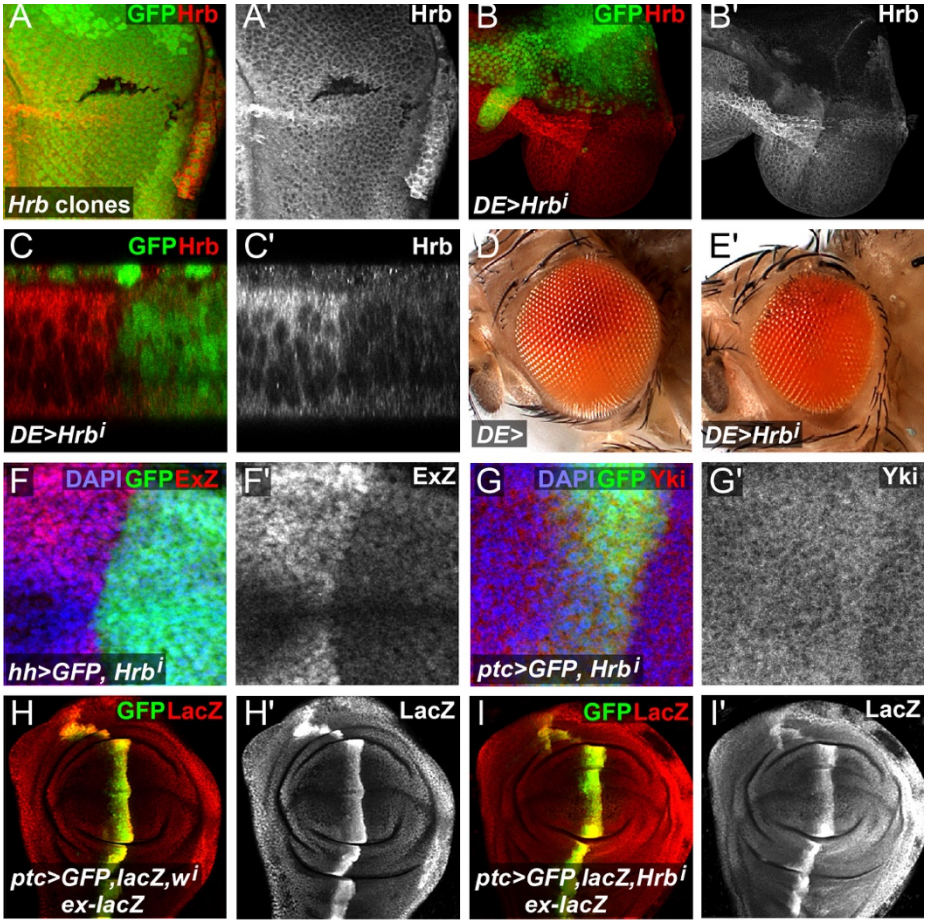

Figure S2. Validation of the *Hrb27C-RNAi* constructs and the Hrb27C antibodies.
(A) Third instar eye disc with negatively GFP marked *Hrb27C*$^{F2\text{-}1}$ mitotic clones stained with anti-Hrb27C to show loss of protein. (B) Third instar eye disc with *Hrb27C-RNAi* and GFP co-expressed in the dorsal region via the *DE-Gal4* driver, stained with anti-Hrb27C antibodies. (C) Higher magnification optical section of the disc in (B), detailing the cellular localization of Hrb27C protein on the left side and the knockdown of *Hrb27C* on the right side. (D) Picture of a control fly with *DE-Gal4* and (E) a fly with *DE-Gal4* driven *Hrb27C-RNAi* in the dorsal compartment of the developing eye. As a result, the dorsal part of the eye was mostly ablated. (F,G) Higher magnification of third instar wing discs expressing (F) *hh-Gal4*, *UAS-GFP* with *Hrb27C-RNAi* stained to detect *ex-lacZ*, and (G) *ptc-Gal4, UAS-GFP* with *Hrb27C-RNAi* stained to detect Yki, and nuclei (DAPI, blue) (H,I) Third instar wing disc expressing *ptc-Gal4*, *UAS-GFP*, *UAS-LacZ* with (H) *white-RNAi*, or (I) *Hrb27C-RNAi*. Discs were stained to detect the expression of the *ex-lacZ* and *UAS-lacZ* (red, grey) and nuclei (DAPI, blue).

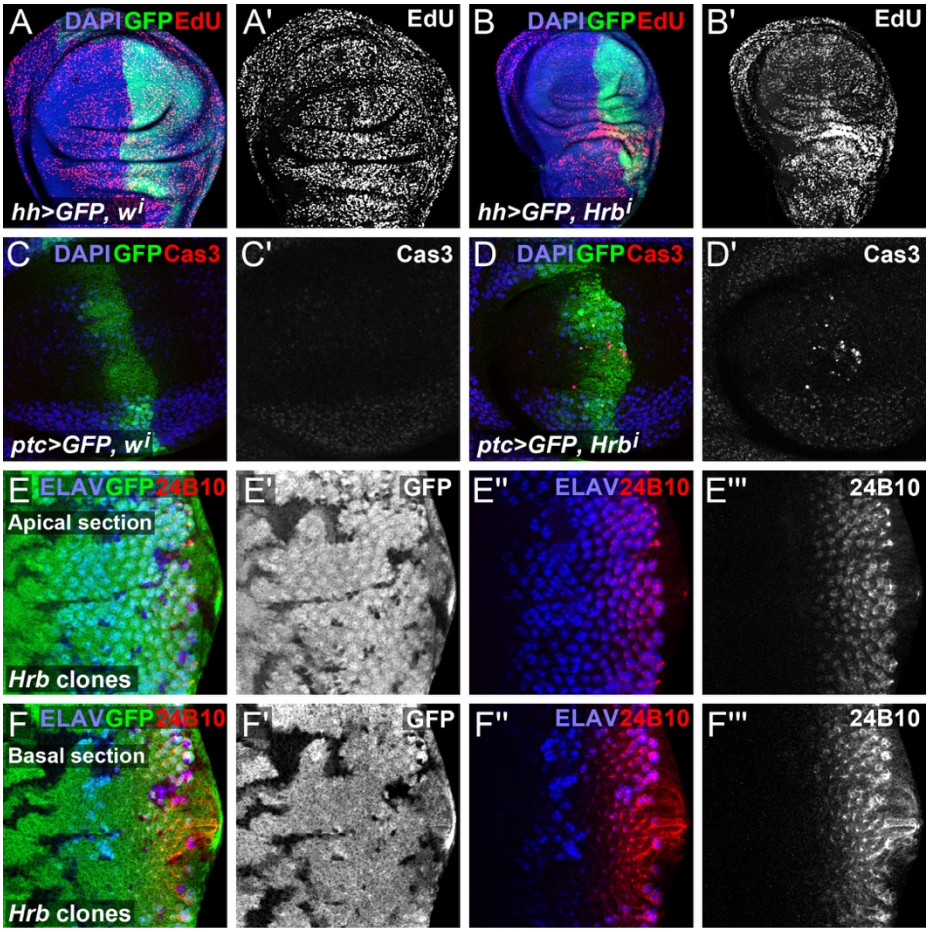

Figure S3. Loss of Hrb27C causes low levels of apoptosis.
(A,B) Wing imaginal discs expressing *hh-Gal4 UAS-GFP* (green) plus (A) *white-RNAi* or (B) *Hrb27C-RNAi.* (C,D) Wing imaginal discs expressing *ptc-Gal4, UAS-GFP* (green) plus (C) *white-RNAi* or (D) *Hrb27C-RNAi.* Discs were stained for EdU incorporation and activated Caspase 3 to detect dividing (EdU, red, grey) and apoptotic cells (Cas3, red, grey); nuclei in blue (DAPI). (E,F) Third instar eye disc with negatively GFP marked $Hrb27C^{F2\text{-}1}$ mitotic clones stained with ELAV (blue) and 24B10 (red, grey).

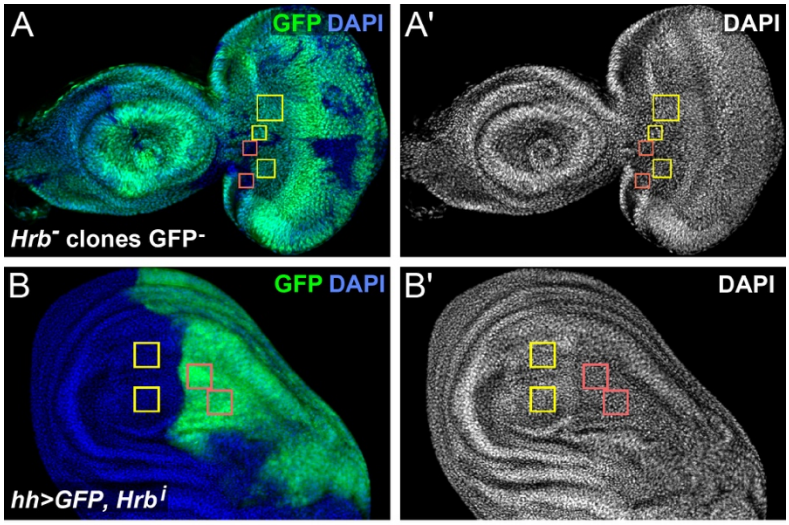

C

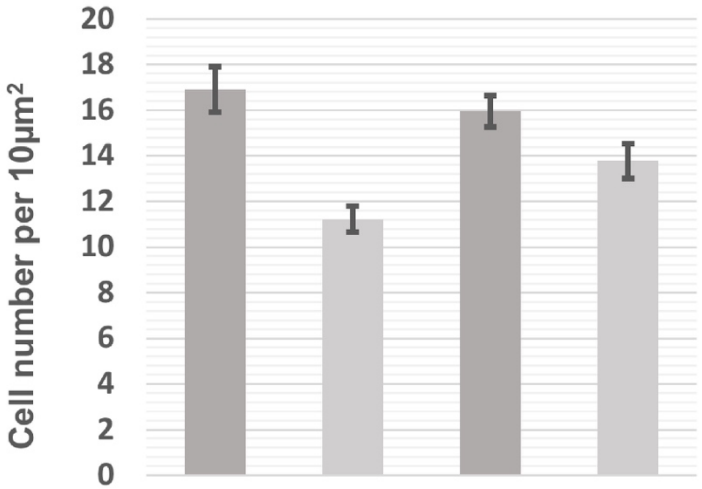

	n = 11	n = 10	n = 13	n = 14
Average	16,92	11,21	15,96	13,77
StdError	0,99	0,58	0,68	0,76

Figure S4. Loss of Hrb27C reduces cell density.
Cell nuclei were manually counted in the Hrb27C deficient and wild type (WT) tissues of imaginal discs: (A) *Hrb27C*^{J6} MARCM clones in the eye imaginal disc (red squares) and wild-type clones (yellow squares) outside the morphogenic furrow, and (B) knock-down of *Hrb27C* by RNAi co-expressed with GFP driven by *hh-Gal4* in the posterior compartment with wild-type tissue in the anterior compartment (yellow squares) within the wing pouch avoiding tissue folds. (C) Absolute values were normalized to get an average nuclei number per 10µm^2 of the imaginal tissue.

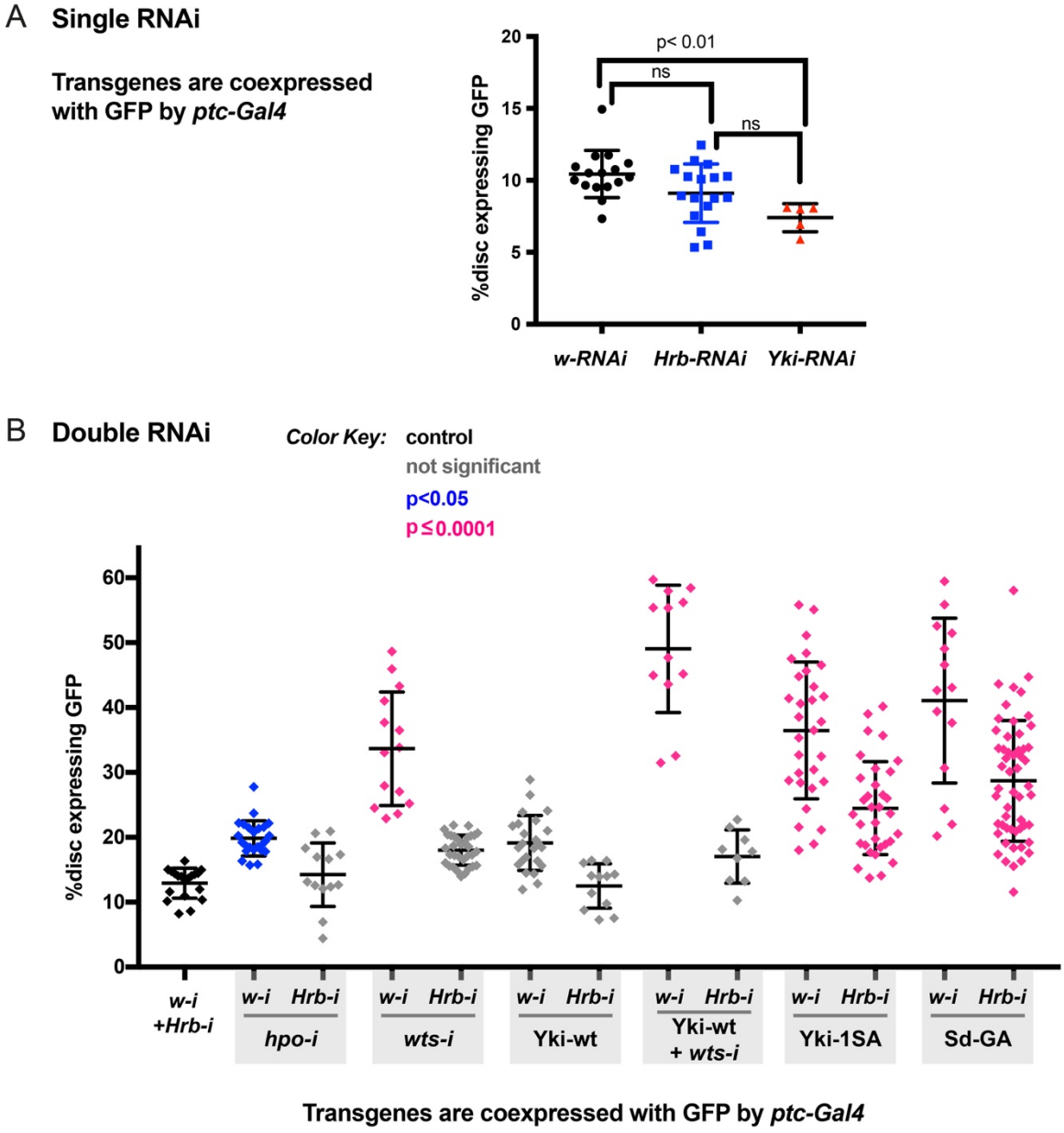

Figure S5. Quantification of the effects of Hrb27C RNAi on Yki driven wing disc growth. Graphs show the relative size of the GFP expressing area compared to size of the entire discs of third instar wing discs expressing various RNAi and overexpression constructs driven by the *ptc-Gal4* driver as is indicated along the x-axes of the two graphs. Representative discs are shown in Figure 4. Error bars indicate standard deviation. In **B**, color coding indicates the significance of the size differences compared to the *white-RNAi + Hrb-RNAi* discs. For both datasets a One Way ANOVA analysis with multiple comparisons test was performed to determine significance. In A, all comparisons were performed. In B, all samples were compared to *white-RNAi+Hrb-RNAi* (black).

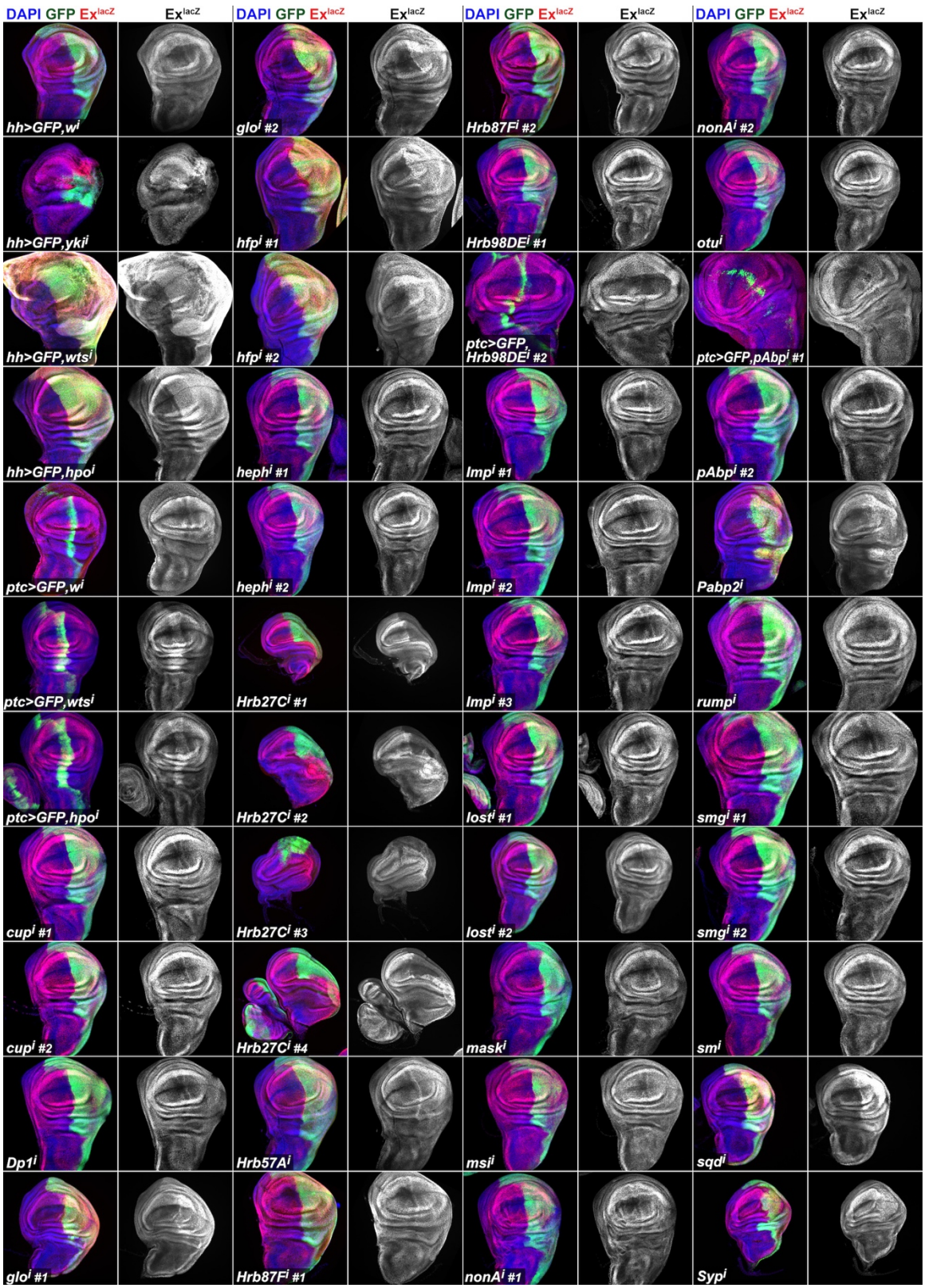
DAPI GFP Ex^lacZ
Ex^lacZ
hh>GFP,w^i
hh>GFP,yki^i
hh>GFP,wts^i
hh>GFP,hpo^i
ptc>GFP,w^i
ptc>GFP,wts^i
ptc>GFP,hpo^i
cup^i #1
cup^i #2
Dp1^i
glo^i #1
glo^i #2
hfp^i #1
hfp^i #2
heph^i #1
heph^i #2
Hrb27C^i #1
Hrb27C^i #2
Hrb27C^i #3
Hrb27C^i #4
Hrb57A^i
Hrb87F^i #1
Hrb87F^i #2
Hrb98DE^i #1
ptc>GFP, Hrb98DE^i #2
Imp^i #1
Imp^i #2
Imp^i #3
lost^i #1
lost^i #2
mask^i
msi^i
nonA^i #1
nonA^i #2
otu^i
ptc>GFP,pAbp^i #1
pAbp^i #2
Pabp2^i
rump^i
smg^i #1
smg^i #2
sm^i
sqd^i
Syp^i

Figure S6. Identification of other RNA binding factors that regulate the output of the Hippo pathway.

In total 37 different RNAi lines for 22 Hrb27C interacting proteins or Hrb27C related RNA binding proteins (5), including four independent RNAi lines for *Hrb27C*, were crossed to *ex-lacZ; hh-Gal4, UAS-GFP* and assessed for the effect on the compartment size and Ex-lacZ levels. Lethal genotypes were re-tested with *ex-lacZ, ptc-Gal4* as indicated. From top to bottom, left to right: *w-RNAi* [Bloomington Stock Centar (BDSC) #25787], *yki-RNAi* [Viena Drosophila Resource Center (VDRC) #104523], *wts-RNAi* (VDRC #106174), *hpo-RNAi* (VDRC #104169), *cup-RNAi #1* (BDSC #26732, *cup-RNAi #2* (BDSC #35406), *Dp1-RNAi* (BDSC #32872), *glo-RNAi #1* (BDSC #36066), *glo-RNAi #2* (VDRC #110653), *hfp-RNAi #1* (BDSC #34785), *hfp-RNAi #2* (BDSC #25951), *heph-RNAi #1* (BDSC #27040), *heph-RNAi #2* (BDSC #35669), *Hrb27C-RNAi #1* (VDRC #16040), *Hrb27C-RNAi #2* (VDRC #16041), *Hrb27C-RNAi #3* (VDRC #101555), *Hrb27C-RNAi #4* (BDSC #33716), *Hrb57A-RNAi* (BDSC #42540), *Hrb87F-RNAi #1* (BDSC #31244), *Hrb87F-RNAi #2* (BDSC #52937), *Hrb98DE-RNAi #1* (BDSC #31303), *Hrb98DE-RNAi #2* (BDSC #32351), *Imp-RNAi #1* (BDSC #34977), *Imp-RNAi #2* (BDSC #38219), *Imp-RNAi #3* (BDSC #55645), *lost-RNAi #1* (BDSC #38931), *lost-RNAi #2* (BDSC #55201), *mask-RNAi* (VDRC #33396), *msi-RNAi* (BDSC #55152), *nonA-RNAi #1* (BDSC-52933), *nonA-RNAi #2* (BDSC #56944), *otu-RNAi* (BDSC #34065), *pAbp-RNAi #1* (BDSC #28821), *pAbp-RNAi #2* (BDSC #36127), *Pabp2-RNAi* (VDRC #106466), *rump-RNAi* (BDSC #42665), *smg-RNAi #1* (BDSC #35477), *smg-RNAi #2* (BDSC #56913), *sm-RNAi* (VDRC #108351), *sqd-RNAi* (VDRC #32395), *Syp-RNAi* (BDSC #56972). Discs were stained to detect the expression of the *ex-lacZ* reporter (Ex^{lacZ}, red, grey) and nuclei (DAPI, blue) as indicated.

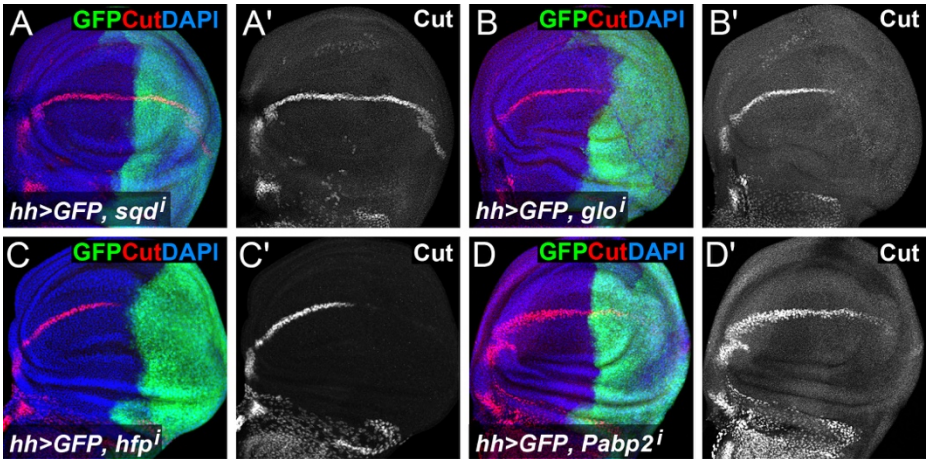

Figure S7. Loss of Glo, Pabp2 and Hfp, but not Sqd, deregulate Notch signaling.
(A-D) Wing imaginal discs expressing *hh-Gal4, UAS-GFP* (green) plus (A) *sqd-RNAi*, (B) *glo-RNAi*, (C) *hfp-RNAi*, and (D) *Pabp2-RNAi*. Discs were stained to detect the expression of Cut (red, grey) and nuclei (DAPI, blue).

Gene	Hrb tartget?	Cell type
Hippo core		
Hpo	No	
Sav	No	
Wts	Yes	S2, TH, elav, pdf
Mats	Yes	elav
Yki	Yes	S2, elav
Sd	No	
Hippo pathway periphery		
Fat	No	
Ds	No	
Fj	No	
Dachs	No	
Lft	No	
Dco	Yes	S2, TH, elav, pdf
App	Yes	TH, pdf
Fbxl7	No	
Mnb	Yes	S2, TH, elav, pdf
Riq	Yes	S2, TH, elav, pdf
Ed	Yes	TH, elav
Ex	No	
Mer	No	
Kibra	No	
Tao	Yes	S2, TH, elav, pdf
Msn	Yes	S2, pdf
RASSF	Yes	S2, TH
Jub	No	
Hipk	Yes	S2, TH, elav, pdf
Mask	Yes	S2, TH, elav, pdf
Wbp2	Yes	TH, elav, pdf
Tgi	No	
Hth	Yes	TH, elav, pdf

Gene	Hrb tartget?	Cell type
Hippo pathway regulators		
STRIPAK	Yes	S2, pdf
PPI	Yes	pdf
Su(DX)	Yes	S2, elav, TH
Slimb	No	
14-4-4	Yes	S2, TH, elav, pdf
Brm	Yes	TH, elav
Ncoa6	Yes	TH
Dsh	Yes	S2
Mad	Yes	S2, TH, pdf
Smox	Yes	S2, TH, elav, pdf
Mop	Yes	pdf
Cell polarity and cell adhesion		
Crb	Yes	S2
aPKC	Yes	S2, TH, elav, pdf
Baz	No	
Par6	No	
Sdt	Yes	S2, TH, elav, pdf
Scrib	Yes	TH, elav
Dlg	Yes	S2, TH, elav, pdf
Lgl	No	
Pez	No	
Patj	No	
a-Catenin	Yes	TH, elav, pdf
b-Cat (arm)	Yes	TH, elav, pdf
ZO-1/2 (pyd)	Yes	S2, elav
E-cad (shg)	Yes	S2, pdf
Zyx	Yes	S2, TH, elav, pdf

Figure S8. Hrb27C mRNA targets of genes in the Hippo pathway.
List of Hippo pathway core components and components acting otherwise in the Hippo pathway and in cell polarity indicating for which genes their mRNA was bound by Hrb27C in different cell types *in vitro* and *in vivo*: Drosophila S2 cells (S2), dopaminergic neurons expressing tyrosine hydroxylase (TH), all differentiated neurons (elav), and the core circadian PDF neuropeptide expressing cells (pdf) (6).

SI References

1. Eder AM, et al. (2005) Atypical PKC contributes to poor prognosis through loss of apical-basal polarity and Cyclin E overexpression in ovarian cancer. *Proceedings of the National Academy of Sciences* 102(35):12519–12524.

2. Morrison CM, Halder G (2010) Characterization of a dorsal-eye Gal4 Line in *Drosophila*. *genesis* 48(1):3–7.

3. Wu JS, Luo L (2007) A protocol for mosaic analysis with a repressible cell marker (MARCM) in Drosophila. *Nature Protocols* 1(6):2583–2589.

4. Sansores-Garcia L, et al. (2013) Mask Is Required for the Activity of the Hippo Pathway Effector Yki/YAP. *Current Biology* 23(3):229–235.

5. Piccolo LL, Corona D, Onorati MC (2014) Emerging Roles for hnRNPs in post-transcriptional regulation: what can we learn from flies? *Chromosoma* 123(6):515–527.

6. McMahon AC, et al. (2016) TRIBE: Hijacking an RNA-Editing Enzyme to Identify Cell-Specific Targets of RNA-Binding Proteins. *Cell* 165(3):742–753.